Numerical study on maneuvering a container ship in shallow water waves

Premchand Mallampalli[1*], Sheeja Janardhanan[2], Kesavadev Varikattu Karottu[3], Gnaneswar Ommi[4]

[1,2,3,4]*School of NAOE, Indian Maritime University, Vangali Village, Sabbavaram Mandal, Visakhapatnam, India.*

Corresponding author: Premchand Mallampalli (*Email: pcmallampalli@imu.ac.in*)

Abstract

Numerous practical and mathematical techniques have been piloted to study ships' behavior in deep water conditions with and without waves, and shallow water conditions without waves, while only limited investigations have been carried out to assess ships' behavior in shallow waters with wave conditions as the flow around the stern region and appendages and the interaction effects are intricate. Therefore, this study attempts to understand the infrequently explored subset of a vessel's behavior in regular waves in shallow water conditions (channel depth to ship draft ratio taken as 1.5). A container ship (S175) model scaled at 1:36 was the subject of a numerical study in which it was subjected to static and dynamic maneuver simulations in head sea conditions. The waves were induced using the dispersion relationship of waves in a given depth. The trends of forces and moments acting on the hull while undergoing maneuvering motions were obtained using a smooth particle hydrodynamics-based computational fluid dynamics solver. The resulting periodic trends of forces and moments were analyzed using the Fourier series method to extract the Fourier coefficients and, in turn, calculate the hydrodynamic derivatives. The trajectories in turning circle and zigzag maneuvers were also simulated using a MATLAB code. The results demonstrate an increase in trajectory parameters and improvement in counter maneuverability owing to the complex flow physics around the hull when encountering regular waves in shallow water conditions compared to waves in deep waters and a lack of waves in shallow waters.

Keywords: CFD, Fourier series, Maneuverability, Regular waves, S175, Shallow water wave conditions, Trajectories.

Authors' Contributions: All authors contributed equally to the conception and design of the study. All authors have read and agreed to the published version of the manuscript.
Competing Interests: The authors declare that they have no competing interests.
Transparency: The authors confirm that the manuscript is an honest, accurate, and transparent account of the study; that no vital features of the study have been omitted; and that any discrepancies from the study as planned have been explained. This study followed all ethical practices during writing.
Institutional Review Board Statement: Not applicable.

1. Introduction

In regular or irregular waves, a vessel at sea is subjected to linear (surge, sway and heave) and rotational (roll, pitch and yaw) motions which constitute the six degrees of freedom. The motions in the horizontal plane (surge, sway and yaw), i.e.

the waterplane/XY plane (see Figure 1 for the coordinate system), are of particular interest as far as the vessel's maneuverability is concerned. The equations of motion of these movements are usually solved to predict the vessel's trajectory using a suitable mathematical model. These hydrodynamic derivatives are intrinsic properties of the ship's underwater hull form and are influenced by the geometry of the hull and attached appendages, the hull-propeller-rudder interaction and the environmental effects. This paper makes an effort to study the influence of waves, a subset of the environmental dynamic forces, on the maneuverability of a hull form in restricted water depths.
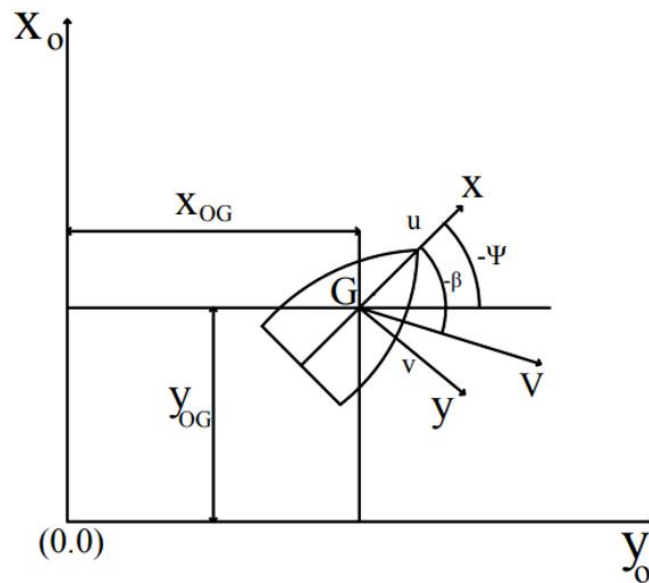

Figure 1.
Earth fixed coordinate system and ship fixed coordinate system.

The objective of the International Maritime Organization (IMO) is to regulate international shipping for the purpose of promoting safer shipping and cleaner oceans. The 71st session of the Marine Environment Protection Committee (MEPC) was concerned with ships' minimum power requirements, maneuverability under adverse weather conditions (i.e., in waves, wind and currents) and stability in waves. The estimation of the maneuvering qualities of the hull form at an early stage of design is the most challenging task, as these require the estimation of various hydrodynamic coefficients (including inertia, damping and restoring terms) to solve the maneuvering equations of motion and predict the vessel's trajectory.

The effects of wavelength and encounter angle to waves, as well as the effect of loading conditions on maneuverability based on experimental data, were studied by Ueno et al. [1], who predicted the vessel's drifting distance and direction. Large drift was observed for short wavelengths, and the drifting direction was observed to differ from the incoming wave direction.

The bare hull forces and vortices around the KRISO Very Large Crude Carrier (KVLCC) tanker hull form during steady drift tests in deep and shallow water were examined by Simonsen et al. [2] and Simonsen and Stern [3]. They demonstrated the variation in hull pressure in shallow water and, in turn, its effect on the hydrodynamic forces in forward motion and static drift. An estimation of a ship's maneuvering performance in waves was obtained using a 3D panel method by Lin et al. [4]. In this study, the maneuvering performance in waves was calculated using the B-spline Rankine panel method.

The effects of wave amplitude and wavelength on the maneuverability of the KVLCC model were studied by Lee et al. [5]; the results indicated that second-order wave force has a dominant influence on turning trajectory and zigzag maneuvers. Studies to determine the velocity-dependent linear and non-linear hydrodynamic coefficients of a container ship by simulating static tests like oblique tests using Reynolds Averaged Navier Stokes Equations (RANSE) for a range of drift angles without waves were carried out by Janardhanan and Krishnankutty [6].

Yasukawa, et al. [7] conducted experiments and measured ship motions in head waves and beam waves and concluded that an increase in hull drift angle influences lateral motions, i.e., sway, roll and yaw, and increases their amplitudes. However, the influence of drift angle on motions like surge, heave and pitch was not remarkable. Moreover, Seo and Kim [8], to predict the maneuvering performance of a hull in waves, derived several methods based on the 2D strip method to estimate wave-induced motion.

As noted by Skejic and Faltinsen [9], there are many technical difficulties related to the analysis of ship maneuvering in waves due to the inadequacy of turbulence models for large angles of attack, cross-flow shed vortices, etc. Subramanian and Beck [10] developed a time-domain body exact strip theory to predict the maneuvering of a vessel in a seaway. They present results for the turning circle maneuver of the containership S-175 in calm water and in the presence of regular waves. The results are compared with available experimental results. The general qualitative aspects of the maneuver are captured by the numerical model, particularly for longer waves. However, the accuracy could drop as wave steepness increases.

Numerical planar motion mechanism (PMM) simulation tests on the container S175 hull form in regular waves in head sea conditions were conducted by Rameesha and Krishnankutty [11]. They showed that the estimated hydrodynamic derivatives display substantial variations in comparison with those in still water, which in turn influence the steady turning and zigzag trajectory parameters. Kim et al. [12] performed scaled KVLCC2 free-running model tests in regular waves. The

effects of wave conditions, such as wave direction, length and height, on the turning trajectories were investigated, and the researchers observed that they were reduced by about half of calm water speeds in head waves, but there was little loss of speed in beam waves. When the wavelength is less than the ship length, drifting distances of trajectories are relatively large. Relative drifting angles between wave propagation direction and trajectory drifting direction are largest when the wavelength equals the ship length.

Ruiz [13] tested the sway, roll and yaw movements of a scaled model of an Ultra Large Container Ship (ULCS) in shallow water conditions (i.e., 50% under keel clearance (UKC)) for a limited combination of drift angles, wave amplitudes and wavelengths. The influence of waves (i.e., sway, roll and yaw) were greater at lower speeds than at higher speeds. Hujae, et al. [14] carried out oblique tests on a fixed Korean Research Institute of Ships and Ocean Engineering (KRISO) container ship (KCS) model in regular waves. Hence, the measured forces represented the sum of hull forces and wave-induced forces.

The KCS hull form was studied to understand its maneuvering performance when the ship operates under normal and propulsion failure conditions during maneuvering in calm water and regular waves [15]. It was observed that propulsion failure had a significant influence on the ship's course-keeping capability, seakeeping performance and maneuverability in a real seaway. The turning behavior of the ship differed considerably according to the presence or absence of propulsion power, which caused substantial changes to not only the turning trajectories but also the critical maneuvering indices. It was revealed that the loss of propulsion power led to noticeable increases in the advance, transfer, and time to turn by 90^0 due to the insufficient rudder lift. It is interesting to note that a 180^0 turn could not be achieved under the propulsion loss condition, indicating the poor turning ability of the ship.

White et al. [16] formulated a new fast-running hybrid method that allowed for the study of maneuvering in regular waves. Multiple numerical methods and force models were used for efficient computation of the total hydrodynamic force acting on a vessel maneuvering in waves. The computational savings of the hybrid method were shown to be appreciable over a comparable simulation using the nonlinear volume of fluid (VOF) method, as it offers an efficiency gain of at least a factor of ten over a VOF method with free surface capturing. The proposed hybrid simulation method was tested in two case studies: maneuvering the Duisburg Test Case hull form and maneuvering the KRISO container ship. The comparable accuracy and reduced computational expense highlighted that the hybrid method is an attractive option for the prediction of ship maneuvering performance in waves.

As per IMO and the Maritime Safety Committee (MSC), at the time of a ship's initial design stage, it is essential to predict the maneuvering characteristics for safe navigation in deep sea and harbor conditions. It is a known fact that hydrodynamic coefficients are intrinsic properties of a hull form and can potentially dictate the ship's trajectory; a detailed study of a ship's performance in both deep sea and harbor conditions is challenging and a large quantity of research has been carried out. However, few studies on harbor conditions have been carried out, aside from the model tests conducted by Ruiz [13] on a scaled model of ULCS for a combination of wave parameters, drift angles and shallow water conditions.

This work proposes a novel methodology for predicting the maneuvering behavior of a hull form in regular waves in shallow water, which represent virtually realistic harbor conditions. The waves were assumed to be regular, non-breaking and propagating in intermediate water depth [as described in Section 2]. The wave parameters, including wave height and frequency, were calculated from the dispersion relationship of water waves for a given water depth. The S175 hull form was subjected to static and dynamic simulations to mimic the typical towing tank maneuvering tests, such as steady drift and PMM tests, using a high-fidelity computational fluid dynamics (CFD) solver. The numerically simulated bare hull forces and moments measured at midship were compared with the published results for deep and shallow calm water conditions. The method espoused in this work was able to replicate the existing published results, proving its efficacy. The studies mentioned above were addressed to predict the maneuverability in deep calm water, shallow calm water and deep-water regular wave conditions. Studies on the effects of restricted water depths on the maneuvering behavior of the hull form in wave conditions are indeed scarce in the available literature. In this context, the present study focuses on predicting the ship's maneuvering behavior and trajectories during maneuvering motions to demonstrate an increase in trajectory parameters and an improvement in counter maneuverability when encountering regular waves in shallow water conditions. The hull form geometry and principal parameters used for the present study are given in Figure 2 and Table 1, respectively.
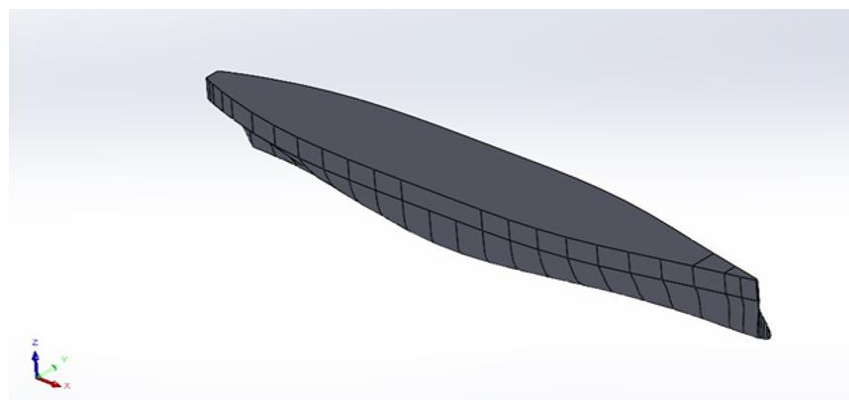

Figure 2.
1:36 3D scaled model of S175.

Table 1.
Principal parameters of S175.

Parameters	Ship	Model
Scale ratio, λ	-	36.000
LBP, L (m)	175.000	4.860
Beam, B (m)	25.400	0.705
Fore draft, T_f (m)	8.000	0.222
End draft, T_a (m)	9.000	0.250
Mean draft, T_m (m)	8.500	0.236
Depth, D (m)	11.000	0.305
Displaced volume, ∇ (m^3)	21.222	0.455
Block coefficient, C_b	0.559	0.559

2. Mathematical Model and CFD Solver

Prediction of ship maneuvering behavior requires a mathematical model representing equations of motion in the horizontal plane. The mathematical model represents a balance of rigid body terms with the hydrodynamic reaction forces and moments. The simplified equations of motion given by Sheeja [17] are represented by Equations 1 through 3.

$$(m - X_{\dot{u}})\dot{u} - X_u \delta u = 0 \tag{1}$$
$$(m - Y_{\dot{v}})\dot{v} - Y_v v + (mx_G - Y_{\dot{r}})\dot{r} + (mu_0 - Y_r)r = 0 \tag{2}$$
$$(mx_G - N_{\dot{v}})\dot{v} - N_v v + (I_z - N_{\dot{r}})\dot{r} + (mx_G u_0 - N_r)r = 0 \tag{3}$$

In the present work, the linear mathematical model proposed by Son and Nomoto [18] and Ruiz [13] has been considered. The non-dimensional factors for forces and moment are $0.5\rho L_m^2 U_m^2$ and $0.5\rho L_m^3 U_m^2$, respectively. The computational domain limits are in line with the International Towing Tank Conference's (ITTC) recommended procedures and guidelines [19] and the prescribed domain size is as per Table 2. The regular wave parameters are computed for intermediate depth (h), where the water depth to draft (h/T_m) ratio is 1.5, wavelength (λ) is assumed as equal to the ship length between perpendiculars (LBP), and the depth to wavelength (h/λ) ratio is 0.0728. From the dispersion relation, the wave frequency is 2.33 rad/sec. The height of the wave is calculated as 0.354m. The ratio of water depth to wavelength ($h/\lambda = 0.0728$) falls into an intermediate depth region, and as a result, waves are assumed to be regular in nature. On the other hand, the size of the ship means that it encounters shallow waters. Hence, the challenge in the present study is to predict the sluggishness of the vessel in shallow depths while encountering waves. The empirical relationships proposed by Son and Nomoto [18] have been simplified and used for rudder and propeller derivatives, as given by Sheeja [17].

Table 2.
Computational domain size.

ITTC recommended (Min.)	Domain		Dimensions (M)
$1.0xL_{BP}$	Upstream	$1.8xL_{BP}$	8.748
$(2-4)xL_{BP}$	Downstream	$3.6xL_{BP}$	17.496
$(0-1)xL_{BP}$	Top	$1.6xL_{BP}$	7.776
h/T < 3.0 (For shallow)	Bottom	h/T=1.5	0.354
$(1-2)xL_{BP}$	Traverse	$2.4xL_{BP}$	11.664

The solver used to carry out the present work is a CFD-based smooth particle hydrodynamics (SPH) code, based on a particle-based Lattice Boltzmann technology. Governing equations in SPH are given in Equations 4 through 10.

The Navier-Stokes equation of flow is given by Equation 4:

$$\frac{dV}{dt} = \frac{-1}{\rho}\nabla p + \frac{\mu}{\rho}\nabla.\nabla V + \frac{1}{\rho}F_{ext} + g \tag{4}$$

Each term in Equation 4 represents acceleration. The discretization term for each term is given by Equations 5 through 7.

The pressure term is

$$\langle\frac{-1}{\rho}\nabla p\rangle_i = \sum_j P_{ij}\nabla W(r_{ij}) \tag{5}$$

where,

$$P_{ij} = -\frac{m_j}{P_j}\left[\frac{p_i}{\rho_i^2} + \frac{p_j}{\rho_j^2}\right] \tag{6}$$

W is known as the weighting or Kernel function.
The viscosity term is represented in Equation 7.

$$\langle\frac{-\mu}{\rho}\nabla.\nabla V\rangle_i = \sum_j V_{ij}\nabla^2 W(r_{ij}) \tag{7}$$

where

$$V_{ij} = -\mu \frac{m_j}{P_j} \left[\frac{v_i}{\rho_i^2} + \frac{v_j}{\rho_j^2} \right] \tag{8}$$

Hence, the total acceleration of the ith particle is given by Equation 9:

$$\frac{dV_i}{dt} = a^{pressure} + a^{viscosity} + a^{external} + a^{gravity} \tag{9}$$

It computes the numerical acceleration of the boundary particles solving the particle interactions with fluid neighboring particles. We assume the same mass for all particles, $m_i = m$. The mass m is calculated by Equation 10.

$$m = \frac{\rho \cdot v}{N} \tag{10}$$

Where v is the total volume of the computational domain and N is the total number of fluid particles. Fluid dynamics computation of forces and pressure are carried out as in Equation 4.

3. Results

To establish the efficacy of the SPH solver, shallow water dynamic simulations as in Sheeja [17] were conducted and were observed to yield reasonably comparable predictions, as shown in Figures 3 and 4. In fact, the computational time and effort for SPH-based CFD was 1.5 times less than that of a typical mesh-based solver.
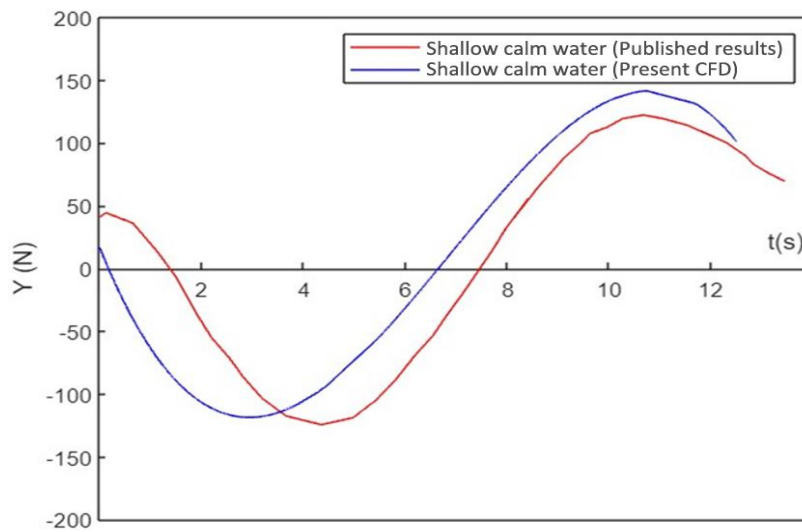

Figure 3.
Comparison of sway forces in a dynamic simulation: present CFD vs published results.
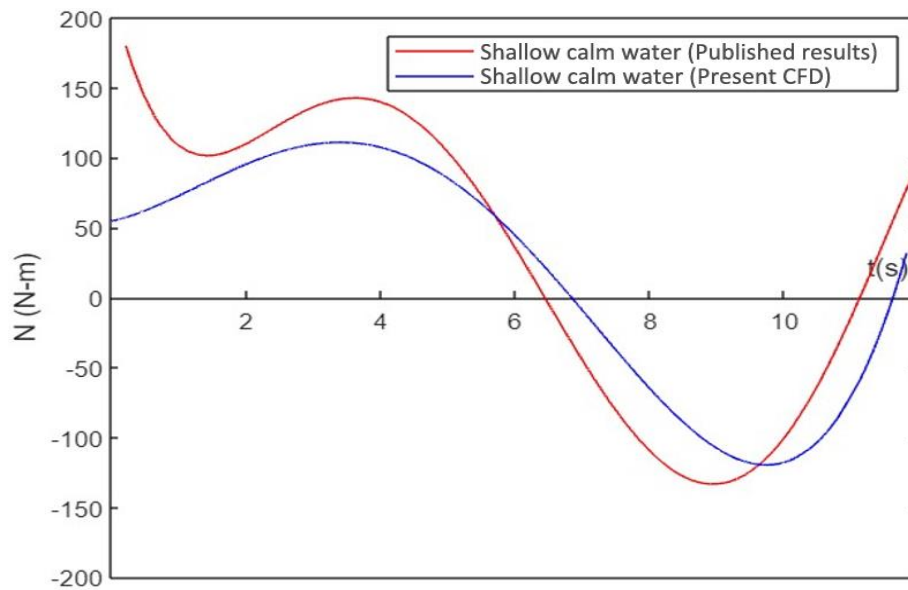**Note:** Sheeja [17].

Figure 4.
Comparison of yaw moment in a dynamic simulation: present CFD vs published results.
Note: Sheeja [17].

The numerically simulated forces and moments measured at midship were non-dimensionalized. The bare hull forces of steady drift were tested in regular waves and dynamic simulations, and the planar motion mechanism (PMM) test was carried out in regular waves. The measured forces and moments were compared with the published results. The present method was able to reproduce the results in the literature, proving its efficacy and reliability. Enhanced forces and moments estimated in the ship's hull in the present study were considered possible contributions by the wave-induced forces and moments on the hull.

3.1. Static Drift Test

In the static drift test, the hull form was oriented at an angle to the centerline of the computational domain (i.e., the drift angle) to the incoming regular waves propagating at a velocity of 1 m/sec. This drift angle leads to asymmetric flow conditions around the hull form. Thus, it behaves like an aerofoil shape to develop lift force and moment. Drift angles were varied from 0 to 10 deg in steps of 2.5 deg. Figure 5 illustrates the free surface elevation during the static drift test.

Computed forces or moments due to the variations in drift angle were plotted against the non-dimensionalized (linear) velocity ($v' = -\sin\beta$) to determine the sway-velocity dependent hydrodynamic derivatives using the higher order curve fitting method, and the results are represented in Table 3 and Figures 6 through 8.
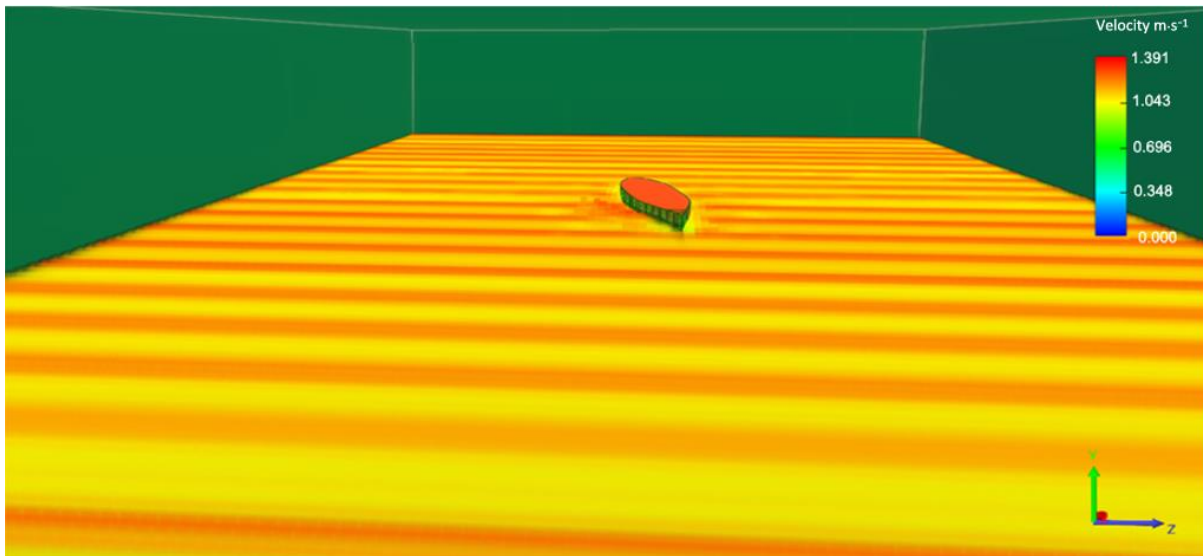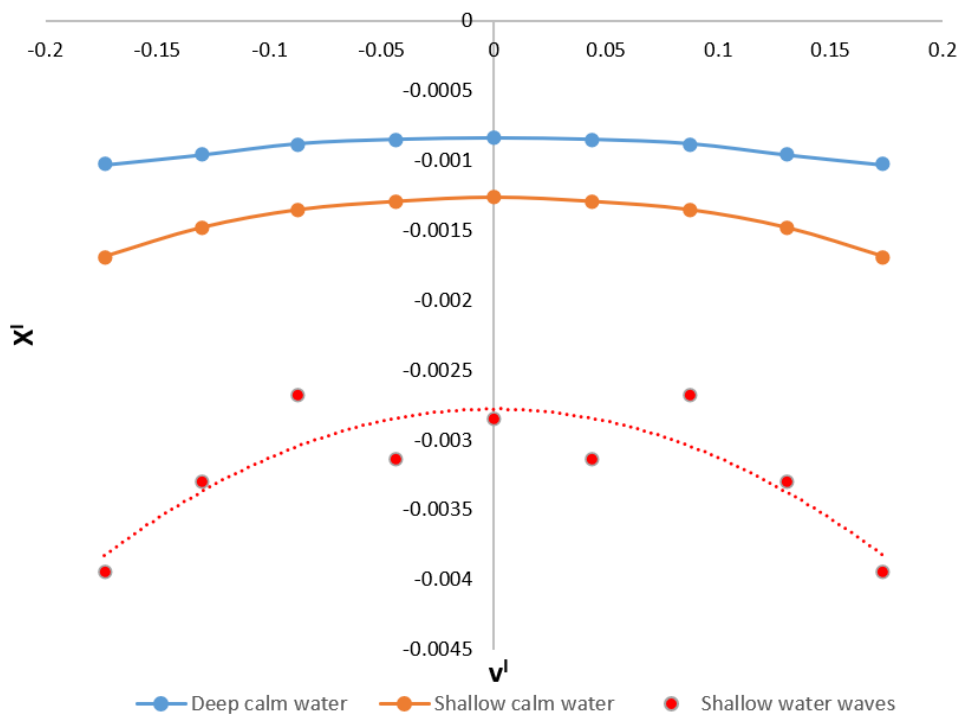

Figure 5.
Water surface captured during drift test.

Figure 6.
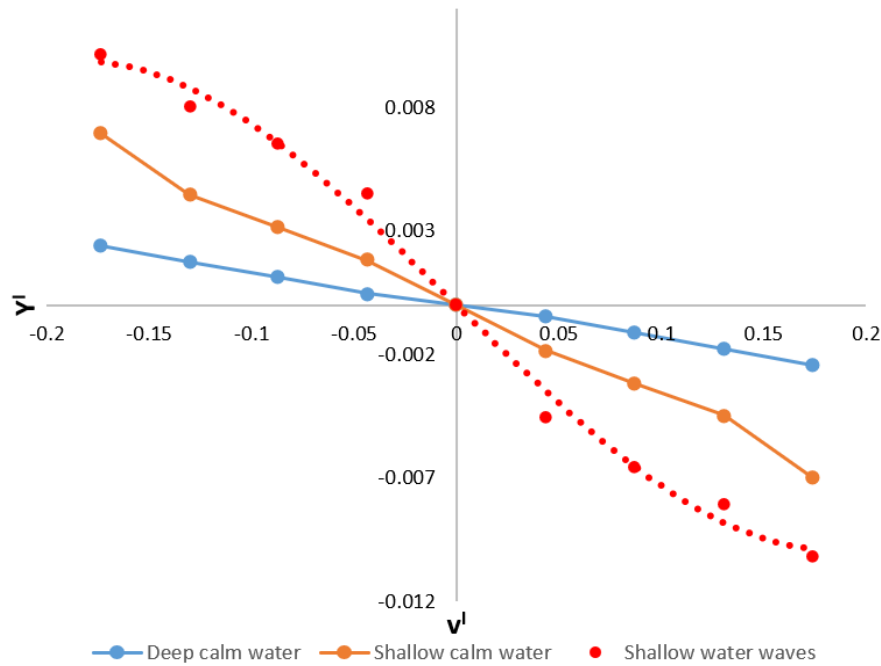Drift test – non-dimensionalized surge force vs velocity.

Figure 7.
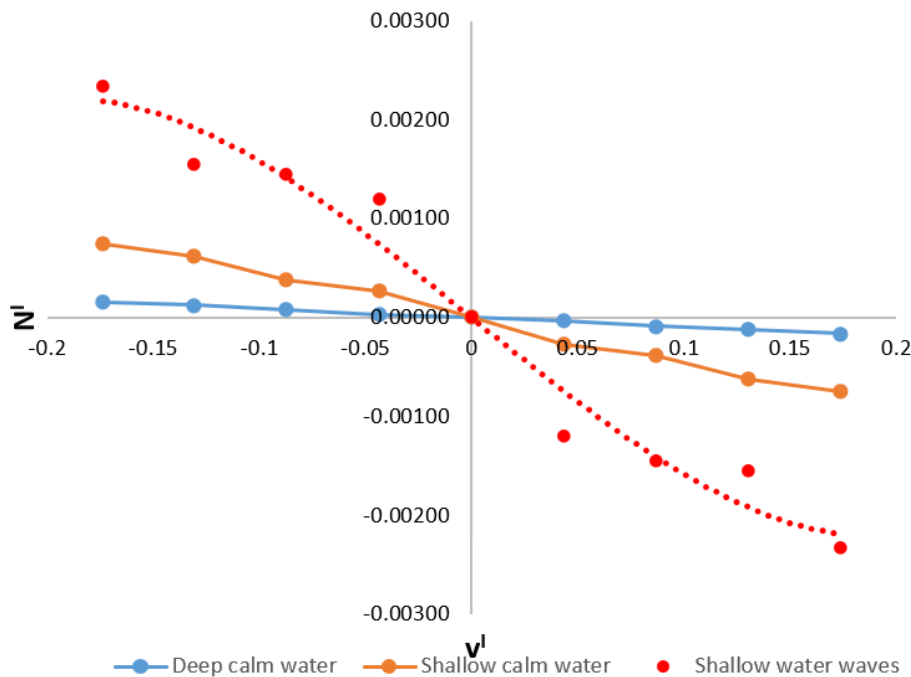Drift test – non-dimensionalized sway force vs velocity.

Figure 8.
Drift test – non-dimensionalized yaw moment vs velocity.

Table 3.
Comparison of sway velocity-dependent derivatives.

Derivative	Deep calm water (Son and Nomoto [18])	Shallow calm water (Sheeja [17])	Shallow water waves (CFD)	Grading (Sheeja [17])
Y_v'	-0.0116	-0.020	-0.0631	A
N_v'	-0.0039	-0.0047	-0.0174	A

3.2. Dynamic Simulations

PMM tests (pure sway and pure yaw) were simulated to compute the hull forces and moments; this data helped to predict the hydrodynamic derivatives using mathematical expressions developed from the Fourier series expansion method. The development of expressions for hydrodynamic derivatives in terms of Fourier coefficients was as in Sheeja [17].

3.2.1. Pure Sway Test

In the pure sway simulation, the hull form considered was defined as a rigid body and subjected to translation motion about the y-axis along the trajectory shown in Figure 9. The hull was subjected to transverse displacement y_o, velocity $\dot{y}_o$ and acceleration $\ddot{y}_o$, as given by Equations 11 through 13. The forward velocity is a non-zero value and forward acceleration, angular (yaw) displacement, velocity and acceleration are zero. By substitution of the above-mentioned values in the mathematical model presented in Equations 1 through 3, the equations of motion are reduced to Equations 14 and 15.

$$\text{Transverse displacement, } y_0 = -y_{0a} \sin \omega t = y \qquad (11)$$
$$\text{Transverse velocity, } \dot{y}_0 = -y_{0a} \omega \cos \omega t = v \qquad (12)$$
$$\text{Transverse acceleration, } \ddot{y}_0 = y_{0a} \omega^2 \sin \omega t = \dot{v} \qquad (13)$$

$$Y_{HY} = Y_{\dot{v}}\dot{v} + Y_v v \qquad (14)$$
$$N_{HY} = N_{\dot{v}}\dot{v} + N_v v \qquad (15)$$

In the present simulation's amplitude of sway oscillations, y_{oa} is taken as 0.3m and the rigid body oscillation frequency ω is taken as 0.47 rad/sec, corresponding to a time period tp of 13.33 sec [17].

3.2.2. Pure Yaw Test

In the pure yaw simulation, the hull form considered was defined as a rigid body and subjected to rotational motion about the z-axis, such that the surge velocity was always tangential to its oscillating path, as shown in Figure 10. The angular displacement, velocity and acceleration are given by Equations 16 through 18. The sway displacement, velocity and acceleration are zero. By substitution of Equations 16 through 18 in the mathematical model, the equations of motion only contain the yaw-dependent terms as shown in Equations 19 through 21.

$$\psi = -\psi_a \cos \omega t \qquad (16)$$
$$\dot{\psi} = r = r_a \sin \omega t \qquad (17)$$
$$\ddot{\psi} = \dot{r} = r_a \cos \omega t \qquad (18)$$

$$X_{HN} = X_{\dot{u}}\dot{u} \qquad (19)$$
$$Y_{HN} = Y_{\dot{r}}\dot{r} + Y_r r \qquad (20)$$
$$N_{HN} = N_{\dot{r}}\dot{r} + N_r r \qquad (21)$$

In the present simulations, the amplitude of yaw angular oscillations ψ_a is taken as 10 deg and the rigid body oscillation frequency ω is taken as 0.47 rad/sec, corresponding to a time period tp of 13.33 sec [17].

The time histories of sway force and yaw moment are plotted in Figures 13 through 16. Using the equations given in Sheeja [17], the Fourier constants were obtained by numerical integration of forces and moments using the trapezoidal rule or Simpson's rule, and consequently, the non-dimensionalized hydrodynamic derivatives were predicted. The predicted hydrodynamic derivatives (for shallow regular wave conditions) were compared with the published results of shallow calm water hull derivatives, as the experimental results for the former data were not available. The effects of the predicted derivatives on various trajectories and maneuvers are given in Table 4.
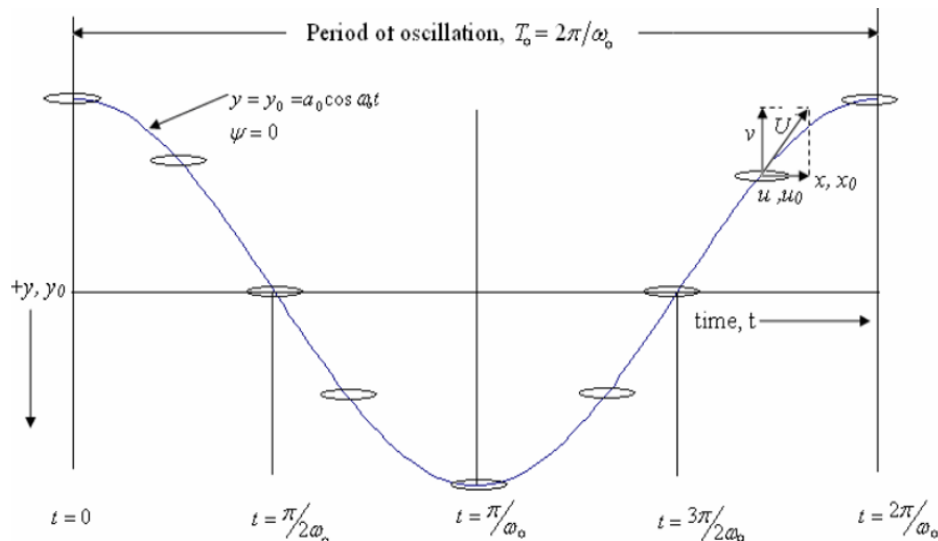

Figure 9.
Pure sway trajectory.
Note: Sheeja [17].

$$\begin{cases} y_0 = -a_0/2[\sin \omega_0 t + \sin(\omega_0 t + \lambda)] \\ \psi = -\psi_0(\cos \omega_0 t - \lambda/2) \end{cases}$$
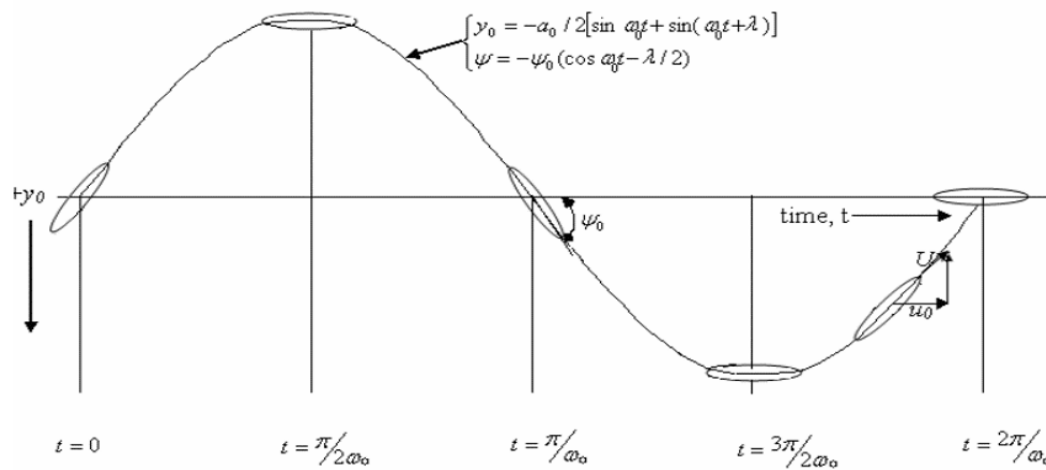
Figure 10.
Pure yaw trajectory.
Note: Sheeja [17].

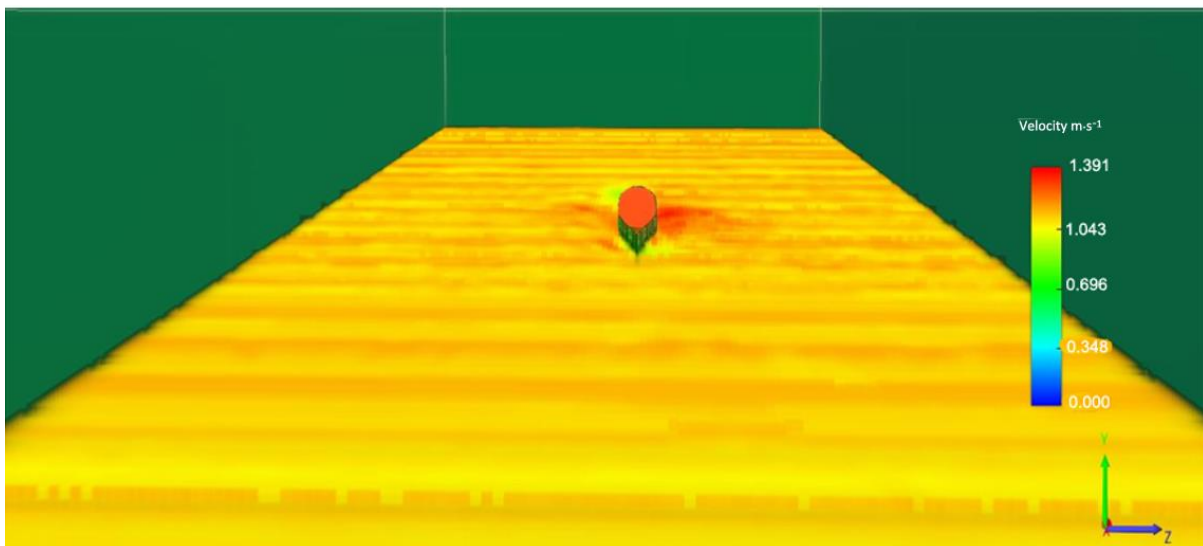Figure 11 illustrates the variation in water surface during the pure sway test.

Figure 11.
Water surface captured during pure sway test.

Figure 12 illustrates the variation in water surface during the pure yaw test.
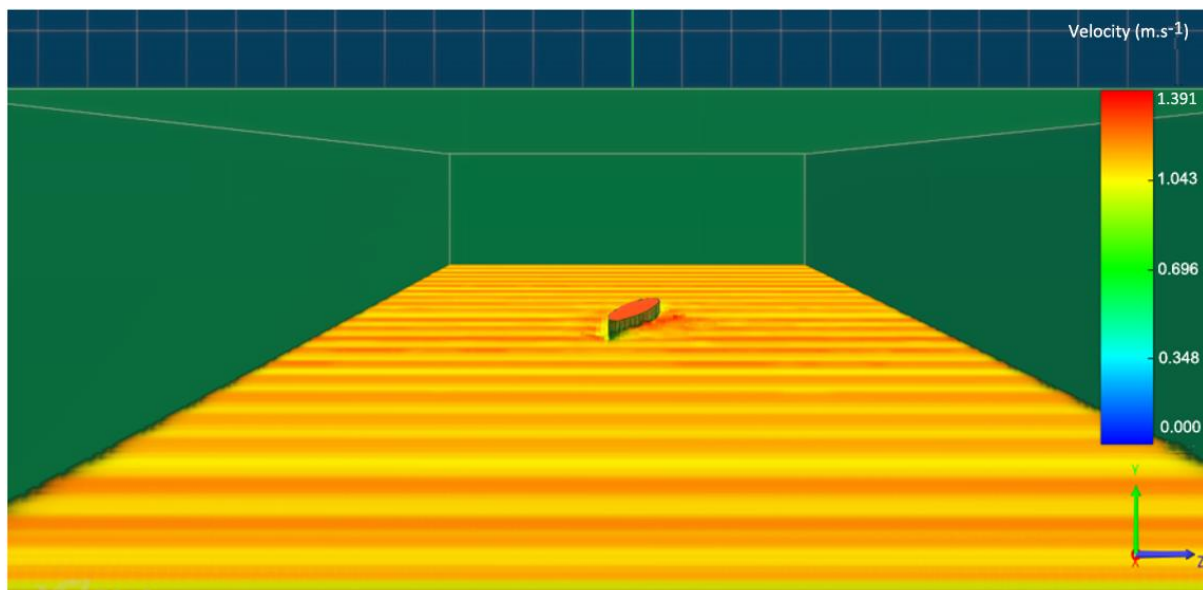

Figure 12.
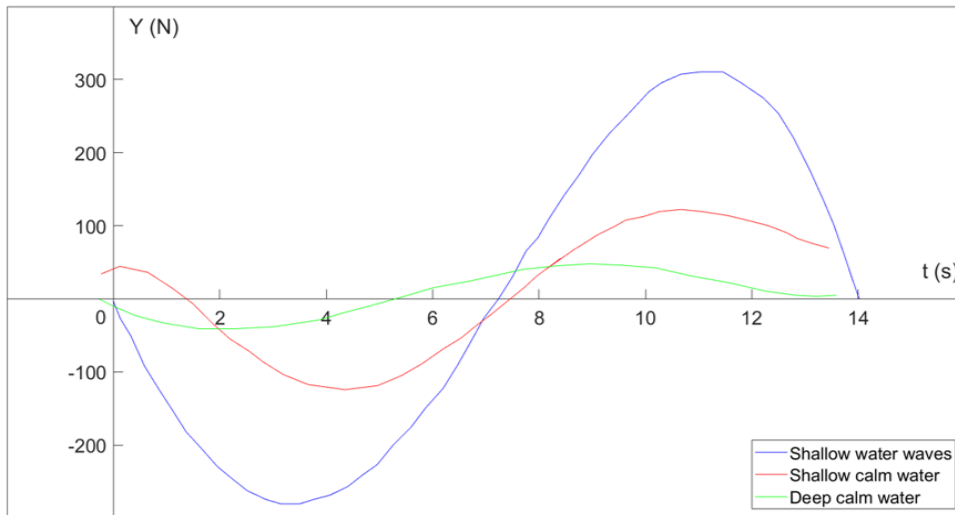Water surface captured during pure yaw test.

Figure 13.
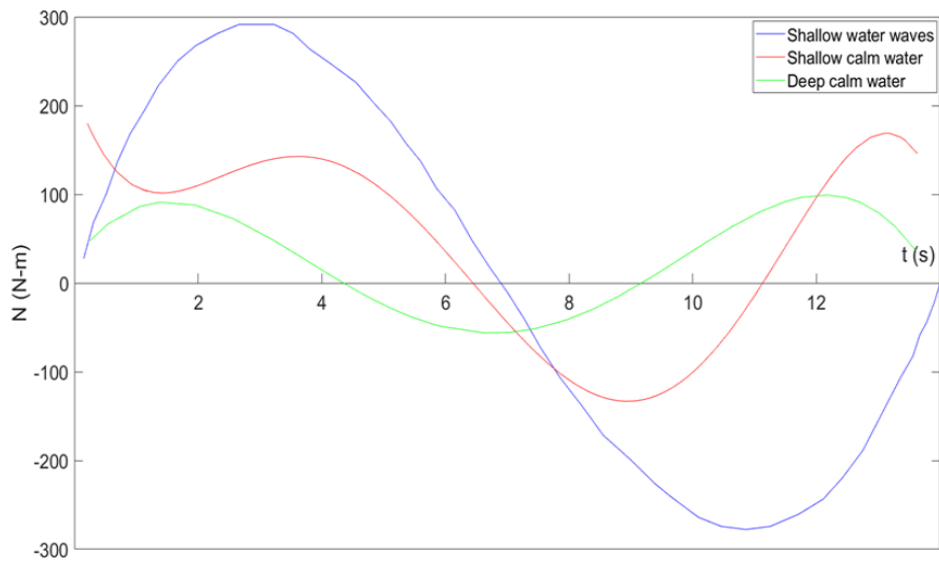Pure sway test – sway force time history.

Figure 14.
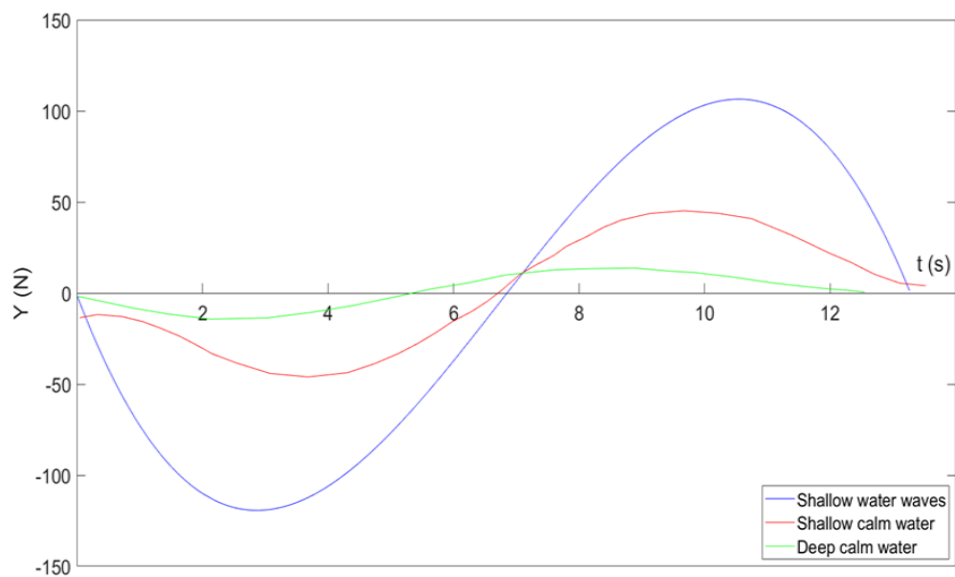Pure sway test – yaw moment time history.

Figure 15.
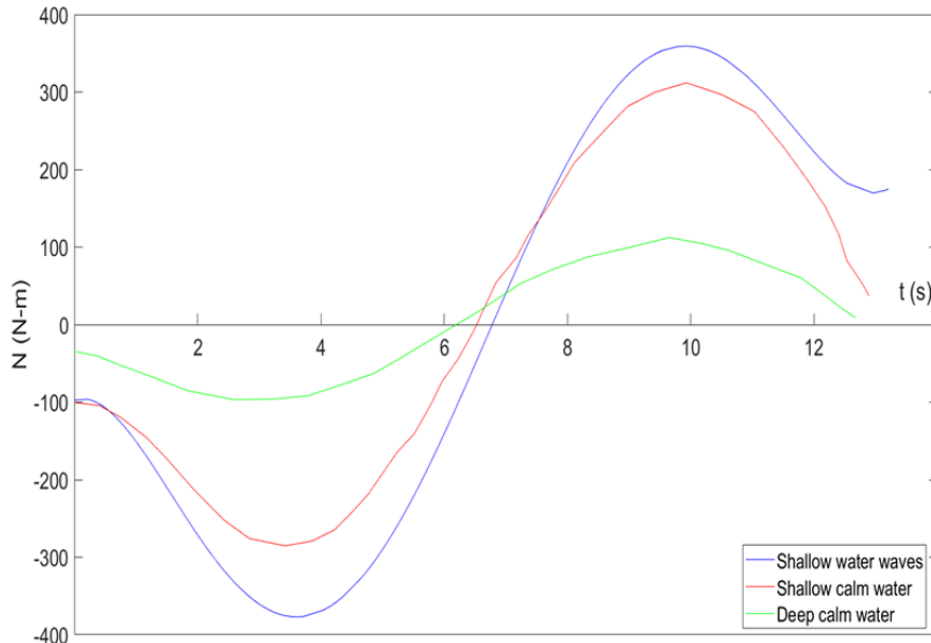Pure yaw test – sway force time history.

Figure 16.
Pure yaw test – yaw moment time history.

Table 4.
Hydrodynamic derivatives predicted from dynamic maneuver simulations in shallow water regular wave conditions.

Derivative	Deep calm water (Son and Nomoto [18])	Shallow calm water (Sheeja [17])	Shallow water waves (CFD)	Grading (Sheeja [17])
Y_v'	-0.0116	-0.0179	-0.05577	A
N_v'	-0.0039	-0.00761	-0.0082	A
$Y_{\dot{v}}'$	-0.007049	-0.01845	-0.03761	A
$N_{\dot{v}}'$	-0.00035	-0.00052	-0.00095	A
$Y_{\dot{r}}'$	-0.00035	-0.00058	-0.00117	A
$N_{\dot{r}}'$	-0.000419	-0.00067	-0.00072	A
N_r'	-0.00222	-0.0065	-0.00964	A
Y_r'	0.00242	0.00783	0.027834	A

The turning circle and zigzag maneuver trajectories were simulated using a Matrix Laboratory (MATLAB) code and were also compared with those observed in shallow calm water simulations, as shown in Figures 17 through 19. Table 5 provides the turning trajectory parameters in shallow calm and shallow wave conditions.
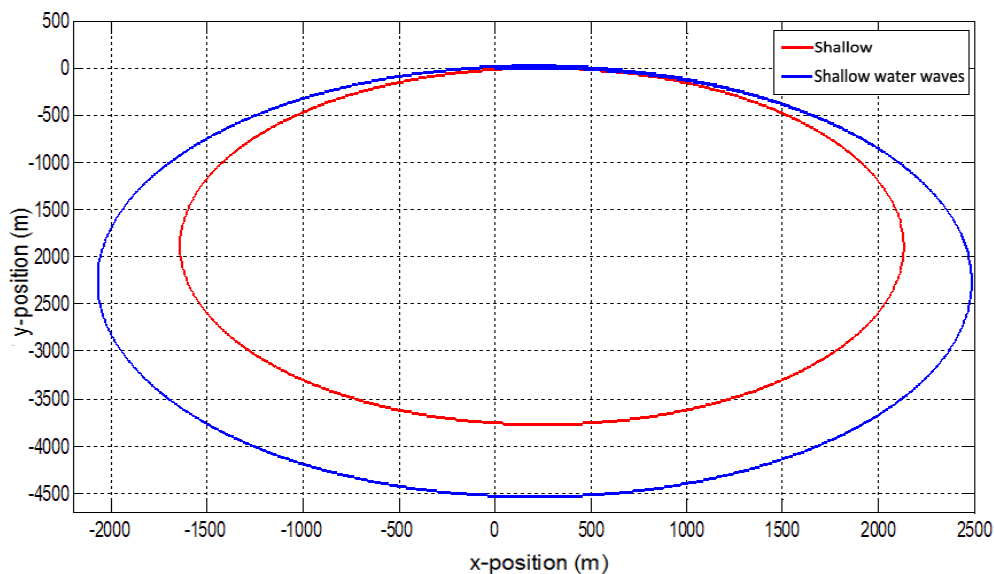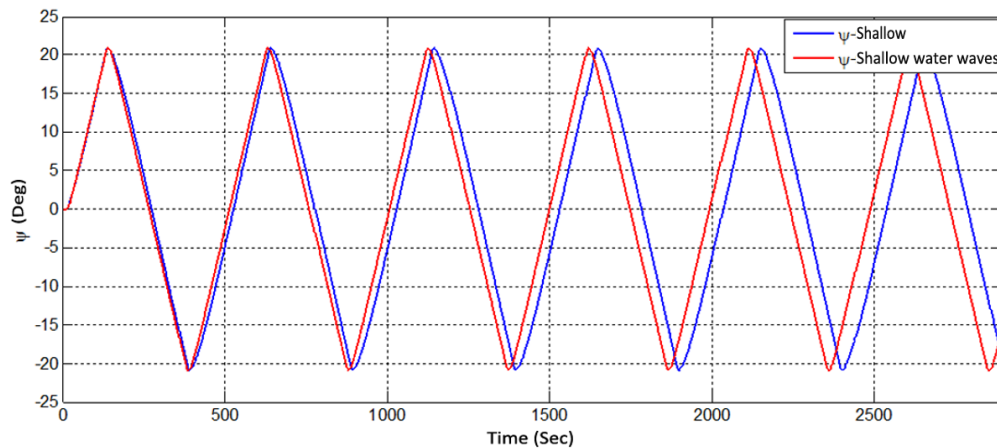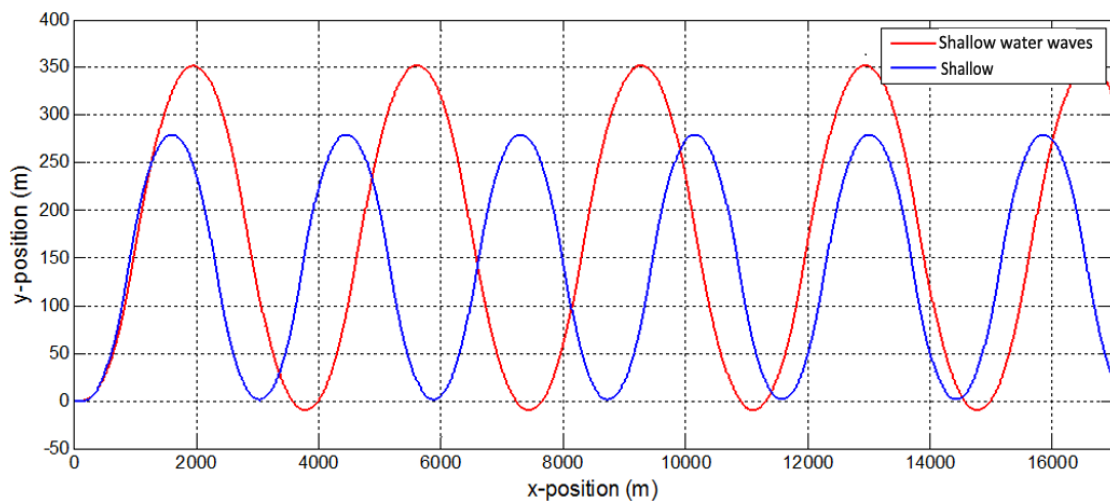

Figure 17.
Turning trajectory in shallow calm and shallow wave conditions.

Table 5.
Turning trajectory parameters in shallow calm and shallow wave conditions.

Turning trajectory parameters	Shallow calm (m)	Shallow wave (m)	Percentage deviation
Rudder execute (X-coordinate)	119	122	
Steady turning radius (m)	1886	2279	20.84
Transfer (m)	1814	2168	19.51
Advance (m)	2012	2363	17.45
Tactical diameter (m)	3773	4536	20.22

Figure 18.
Z-maneuver in shallow calm vs shallow wave conditions.

Figure 19.
Yaw width in shallow calm vs shallow wave conditions.

4. Discussion

The results presented by Janardhanan and Krishnankutty [6] conveyed the effect of water depth on hull form maneuvering behavior, and the results discussed by Rameesha and Krishnankutty [11] concerning regular waves were limited to deep water conditions only. The present study, therefore, attempted to assess the effect of water depth on hull form maneuvering behavior in regular waves in head sea shallow water conditions. In static and dynamic simulations, it is clear that the water depth impacts the hydrodynamic derivatives, which translates to an increase in standard trajectory parameters, as reported by Janardhanan and Krishnankutty [6], while the influence of regular waves in head sea shallow water conditions leads to a further augmentation of hydrodynamic derivatives, which has the following repercussions:

- Inclusive improvement in directional stability
- Approximate enhancement of 20% in turning trajectory parameters
- Improvement in counter maneuverability as hypothesized from the zigzag maneuver simulations

The results presented in Figures 13 through 19 postulate the impact of water depth and wave force on the hydrodynamic derivatives. The time dependency of hydrodynamic derivatives in waves has been neglected in this study. Investigations have been carried out into the augmented forces and moments acting on the hull during maneuvering motions in waves. The hydrodynamic derivatives evaluated through a Fourier series method as in Sheeja [17] are considered to be constants as the amplitude of the waves is considered to be small and the waves to be linear.

5. Conclusions

The present work can be protracted to predict the effect of wave parameters and wave propagation directions on the maneuvering performance of a vessel's hull form; therefore, it can improve our understanding of the hull form's performance in a restricted environment, since the maneuverability of a vessel is of paramount importance in the early design stages.

CFD-based smooth particle hydrodynamics has both qualitatively and quantitatively proved its efficacy in predicting a ship's maneuverability in shallow water with waves. Such predictions are crucial as they offer realistic predictions, leaving the helmsman with a good idea of what to expect when maneuvering the vessel in a harbor or restricted environment.

The present work is a first step towards the study of the influence of regular waves in shallow water on a hull form's maneuvering behavior in three degrees of freedom, neglecting the roll effect using a meshless numerical technique. The present study could be extended to study the effects of irregular waves and other environmental factors, such as wind and current, on maneuvering behavior. In addition, the study could be extended to investigate the different sea state and Beaufort scale conditions for a four-degree-of-freedom model with roll effect, as container ships are susceptible to roll as well. Furthermore, the time dependency of hydrodynamic derivatives in shallow water irregular waves warrants further study.

Nomenclature

M	Body mass/integer for determining harmonic of Fourier series.
$X_{\dot{u}}$	Hydrodynamic uncoupled derivative in surge force with respect to surge acceleration.
X_u	Hydrodynamic linear uncoupled derivative of surge force with respect to sway velocity.
$Y_{\dot{v}}$	Hydrodynamic uncoupled derivatives in sway force with respect to sway acceleration.
Y_v	Hydrodynamic linear uncoupled derivatives of sway force with respect to sway velocity.
U	Forward velocity in ship-fixed coordinate system.
$\dot{u}$	Surge acceleration.
V	Sway velocity in ship-fixed coordinate system.
$\dot{v}$	Sway acceleration.
u_0	Forward velocity in earth-fixed coordinate system.
X_G	Distance of origins of earth and ship fixed coordinate systems.
Y	Forces in transverse direction in ship-fixed coordinate system.
Y_0	Transverse displacement.
$\dot{y}_0$	Transverse velocity.
$\ddot{y}_0$	Transverse acceleration.
Y	Position in transverse direction in ship-fixed coordinate system.
Y_{0a}	Amplitude of sway motion.
ω	Specific dissipation of energy per unit volume.
δ	Rudder angle.
ψ	Heading/yaw angle.
$\dot{\psi}$	Yaw rate.
$\ddot{\psi}$	Yaw acceleration.
ψ_a	Amplitude of yaw angular motion.
T	Instantaneous time.
N_v	Non-dimensional hydrodynamic linear coupled derivative of yaw moment with respect to sway velocity.
$N_{\dot{v}}$	Non-dimensional hydrodynamic coupled derivative of yaw moment with respect to sway acceleration.
R	Yaw rate.
$\dot{r}$	Yaw acceleration.
r_a	Amplitude of yaw rate.
Y_r	Hydrodynamic linear coupled derivative of sway force with respect to yaw rate.
$Y_{\dot{r}}$	Hydrodynamic coupled derivative of sway force with respect to yaw acceleration.
N_r	Hydrodynamic linear uncoupled derivative of yaw moment with respect to yaw rate.
$N_{\dot{r}}$	Hydrodynamic uncoupled derivative of yaw moment with respect to yaw acceleration.
I_z	Mass moment of inertia about the z-axis.
X_{HN}	Hydrodynamic reaction force of surge in pure yaw mode.
Y_{HN}	Hydrodynamic reaction force of sway in pure yaw mode.
Y_{HY}	Hydrodynamic reaction force of sway in pure sway mode.
N_{HN}	Hydrodynamic reaction moment in yaw in pure yaw mode.
N_{HY}	Hydrodynamic reaction moment in yaw in pure sway mode.
V	Velocity field.
ρ	Fluid density.
p	Fluid pressure.
μ	Dynamic viscosity of the fluid.
F_{ext}	External force.
G	Acceleration due to gravity.

References

[1] M. Ueno, T. Nimura, and H. Miyazaki, "Experimental study on manoeuvring motion of a ship in waves," presented at the International Conference on Maritime Simulation and Ship Maneuvering, 2003.

[2] C. D. Simonsen, F. Stern, K. Agdrup, and M. I. W. Barentsz, "CFD with PMM test validation for manoeuvring VLCC2 tanker in deep and shallow water," presented at the In International Conference on Marine Simulation and Ship Manoeuvring (MARSIM), Terschelling, The Netherlands, 2006.

[3] C. D. Simonsen and F. Stern, "Flow structure around maneuvering tanker in deep and shallow water," 26th ONR Symposium on Naval Hydrodynamics, Rome, Italy, 2006.

[4] W.-M. Lin, S. Zhang, and K. Weems, "Numerical simulations of ship maneuvering in waves," in *Proceedings of 26th ONR Symposium on Naval Hydrodynamics, Rome, Italy*, 2006.

[5] S. K. Lee, S. H. Hwang, S. W. Yun, K. P. Rhee, and W. J. Seong, "An experimental study of a ship maneuverability in regular waves," in *Proceedings of the International Conference on Marine Simulation and Ship Maneuverability (MARSIM 2009), Panama*, 2009.

[6] S. Janardhanan and P. Krishnankutty, "Estimation of sway velocity-dependent hydrodynamic derivatives in surface ship manoeuvring using ranse based CFD," *The International Journal of Ocean and Climate Systems,* vol. 1, no. 3-4, pp. 167-178, 2010. https://doi.org/10.1260/1759-3131.1.3-4.167

[7] H. Yasukawa, F. Amri Adnan, and K. Nishi, "Wave-induced motions on a laterally drifting ship," *Ship Technology Research,* vol. 57, no. 2, pp. 84-98, 2010. https://doi.org/10.1179/str.2010.57.2.001

[8] M.-G. Seo and Y. Kim, "Effects of ship motion on ship maneuvering in waves," presented at the 26th International Workshop on Water Waves and Floating Bodies, Greece, 2011.

[9] R. Skejic and O. Faltinsen, "Maneuvering behavior of ships in irregular waves," in *Proceedings of the International Conference on Offshore Mechanics and Arctic Engineering - OMAE*, 2013, vol. 9.

[10] R. Subramanian and R. F. Beck, "A time-domain strip theory approach to maneuvering in a seaway," *Ocean Engineering,* vol. 104, pp. 107-118, 2015. https://doi.org/10.1016/j.oceaneng.2015.04.071

[11] T. Rameesha and P. Krishnankutty, "Numerical study on the manoeuvring of a container ship in regular waves," *Ships and Offshore Structures,* vol. 14, no. 2, pp. 141-152, 2019. https://doi.org/10.1080/17445302.2018.1482706

[12] D. J. Kim, K. Yun, J.-Y. Park, D. J. Yeo, and Y. G. Kim, "Experimental investigation on turning characteristics of KVLCC2 tanker in regular waves," *Ocean Engineering,* vol. 175, pp. 197-206, 2019. https://doi.org/10.1016/j.oceaneng.2019.02.011

[13] M. T. Ruiz, "Wave effects on the turning ability of an ultra large container ship in shallow water," in *Proceedings of the International Conference Offshore Mech. Arct. Eng. - OMAE*, 2019, vol. 7A-2019.

[14] C. Hujae, J. K. Dong, G. K. Yeon, J. Y. Dong, Y. Kunhang, and J. L. Gyeong, "An experimental study on the captive model test of KCS in regular waves," presented at the 5th MASHCON International Conference on Ship Manoeuvring in Shallow and Confined Water with Non-Exclusive Focus on Manoeuvring in Waves, Wind and Current, Ostend, Belgium, 2019.

[15] D. Kim, S. Song, T. Sant, Y. K. Demirel, and T. Tezdogan, "Nonlinear URANS model for evaluating course keeping and turning capabilities of a vessel with propulsion system failure in waves," *International Journal of Naval Architecture and Ocean Engineering,* vol. 14, p. 100425, 2022. https://doi.org/10.1016/j.ijnaoe.2021.11.008

[16] P. F. White, D. J. Piro, B. G. Knight, and K. J. Maki, "A hybrid numerical framework for simulation of ships maneuvering in waves," *Journal of Ship Research,* vol. 66, no. 02, pp. 159-171, 2022. https://doi.org/10.5957/josr.06200037

[17] J. Sheeja, *Numerical estimation of hydrodynamic derivatives in surface ship maneuvering*. Madras: Indian Institute of Technology, 2010.

[18] K. Son and K. Nomoto, "On the coupled motion of steering and rolling of a high speed container ship," *Journal of the Society of Naval Architects of Japan,* vol. 1981, no. 150, pp. 232-244, 1981. https://doi.org/10.2534/jjasnaoe1968.1981.150_232

[19] ITTC, "ITTC-Recommended Procedures and Guidelines Guideline on Use of RANS Tools for Manoeuvring Prediction ITTC Quality System Manual Recommended Procedures and Guidelines Guideline Guideline on Use of RANS Tools for Manoeuvring Prediction Guideline on Use of RANS Tools for Manoeuvring Prediction," 2017. Retrieved from https://www.ittc.info/media/8173/75-03-04-01.pdf.